Received: 23 April 2021 | Accepted: 17 October 2022

DOI: 10.1002/edn3.381

Environmental DNA
Open Access
Dedicated to the study and use of environmental DNA for basic and applied sciences

WILEY

SPECIAL ISSUE ARTICLE

Interspecific allometric scaling in eDNA production among northwestern Atlantic bony fishes reflects physiological allometric scaling

Matthew C. Yates[1] | Taylor M. Wilcox[2] | M. Y. Stoeckle[3] | Daniel D. Heath[1]

[1]University of Windsor, Windsor, Ontario, Canada

[2]National Genomics Center for Wildlife and Fish Conservation, Rocky Mountain Research Station, Missoula, Montana, USA

[3]The Rockefeller University, New York, New York, USA

Correspondence
Matthew C. Yates, University of Windsor, Windsor, Ontario, Canada.
Email: matthew.yates@outlook.com

Abstract

Relating environmental DNA (eDNA) signal strength to organism abundance requires a fundamental understanding of eDNA production. A number of studies have demonstrated that eDNA production may scale allometrically—that is, larger organisms tend to exhibit lower mass-specific eDNA production rates, likely due to allometric scaling in key processes related to eDNA production (e.g., surface area, excretion/egestion). While most previous studies have examined intraspecific allometry, physiological rates and organism surface area also scale allometrically across species. We therefore hypothesize that eDNA production will similarly exhibit interspecific allometric scaling. To evaluate this hypothesis, we reanalyzed previously published eDNA data from Stoeckle et al. (ICES Journal of Marine Science, 78(1), 293–304, 2021) which compared metabarcoding read count to organism count and biomass data obtained from trawl surveys off the New Jersey coast. Using a Bayesian model, we empirically estimated the value of the allometric scaling coefficient ("b") for Northwestern Atlantic bony fishes to be 0.77 (credible interval = 0.64–0.92), although our model failed to converge for Chondrichthyan species. We found that integrating allometry significantly improved correlations between organism abundance and metabarcoding read count relative to traditional metrics of abundance (density and biomass) for bony fishes. Although substantial unexplained variation remains in the relationship between read count and organism abundance, our study provides evidence that eDNA production may scale allometrically across species in some contexts. Future studies investigating the relationship between eDNA signal strength and metrics of fish abundance could potentially be improved by accounting for allometry; to this end, we developed an online tool that can facilitate the integration of allometry in eDNA/abundance relationships.

KEYWORDS
abundance, allometric scaling, allometry, biomass, eDNA, fishes

1 | INTRODUCTION

A consensus is emerging that the relationship between the amount of DNA in an environment (environmental DNA, or "eDNA") tends to be positively correlated with the abundance of organisms within that environment (Rourke et al., 2021; Yates et al., 2019; Yates, Cristescu, & Derry, 2021). The concentration of eDNA can therefore provide information on the "unseen" abundance of organisms and could represent a powerful tool for understanding aquatic community composition. However, studies in natural ecosystems exhibit substantial variation in the strength of the correlation between eDNA concentration and estimated organism abundance, likely because a number of abiotic and biotic variables can affect steady-state concentrations of eDNA (Yates, Cristescu, & Derry, 2021). Improving the capacity to infer abundance from eDNA data therefore requires a better understanding of the "ecology" of eDNA—that is, factors influencing the production, transport, and degradation of nucleic acids in the environment (Barnes & Turner, 2016; Yates, Cristescu, & Derry, 2021).

A number of previous studies have demonstrated that eDNA production likely scales allometrically with body size; that is, as the body mass of an individual increases, their *mass-specific* eDNA production rate (i.e., production rate of eDNA per gram of body mass) tends to decline (Maruyama et al., 2014; Stoeckle et al., 2021; Takeuchi et al., 2019; Yates, Glaser, et al., 2021; Yates, Wilcox, et al., 2021). The primary mechanisms driving this relationship are likely related to long-recognized allometric scaling in the relationship between body mass and surface area (Meeh, 1879; O'Shea et al., 2006), as well as allometric scaling in key physiological rates related to eDNA production (e.g., consumption, excretion, egestion) (Allegier et al., 2015; Post et al., 1999; Vanni & McIntyre, 2016; Yates, Glaser, et al., 2021). Most of the previous studies examining allometry in eDNA production, however, have focused on *intra*specific allometry, quantifying how eDNA production changes as body mass increases *within* a species using single-species assays that estimate the concentration of eDNA in an environment using quantitative PCR (qPCR) or digital droplet PCR (ddPCR) methods. However, metabolic theory postulates that allometry in key physiological rates also operates at an *inter*specific scale; organisms from small-bodied species have, on average, higher physiological rates (Allegier et al., 2015; Brown et al., 2004; Vanni & McIntyre, 2016) and the relationship between body mass and surface area also exhibits interspecific allometry (Meeh, 1879; Reynolds, 1996). Environmental DNA production may therefore be affected by allometry on an *inter*specific basis, as well (Yates, Glaser, et al., 2021). However, the extent to which the distribution of eDNA varies interspecifically with organism abundance and body mass remains relatively understudied.

Metabarcoding approaches, when applied to eDNA samples, can be used to quantify community species composition (Taberlet et al., 2012). When metabarcoding techniques are applied to eDNA samples, primers targeting genomic regions that tend to be conserved across taxonomic groups are used to amplify variable intervening regions. The resulting amplicons are then sequenced on high-throughput sequencing (HTS) platforms to produce millions of reads that are compared to a reference database for taxonomic identification (Cristescu, 2014; Taberlet et al., 2012). However, relationships between metabarcoding sequence count and organism abundance are likely to be weaker than for single-species approaches that directly quantify template eDNA concentrations due to differences in amplification efficiency across taxonomic groups and biases associated with community composition (Kelly et al., 2019; Piñol et al., 2019; Yates, Cristescu, & Derry, 2021). Nevertheless, consistent positive correlations between metabarcoding data and relative species abundance have been observed in controlled and natural settings (Evans et al., 2016; Hanfling et al., 2016; Lawson Handley et al., 2019), highlighting its potential utility to infer abundance even if only qualitative or relative abundance comparisons are possible (Kelly et al., 2019; Lamb et al., 2019; Rourke et al., 2021; Yates, Cristescu, & Derry, 2021).

Relationships between quantitative eDNA metabarcoding data and organism abundance could potentially be further strengthened by applying our growing understanding of the "ecology of eDNA" in natural ecosystems. By integrating eDNA dynamics into modeling efforts, researchers may be able to account for some of the unexplained variation in relationships between eDNA signal strength estimated by metabarcoding and organism abundance in nature (Yates, Cristescu, & Derry, 2021). A better understanding of processes involved in eDNA production, for example, could help improve our understanding of the distribution of eDNA observed among species in natural ecosystems.

Metabarcoding datasets derived from sampling natural ecosystems that are paired with simultaneous observational estimates of organism abundance represent a valuable opportunity to empirically estimate how eDNA production scales across species in natural ecosystems. Here, we analyzed data previously published in Stoeckle et al. (2021), which paired eDNA metabarcoding data with traditional trawl data from the coast of New Jersey (Northwest Atlantic) and empirically estimated the rate at which recovered metabarcoding reads from eDNA samples was impacted by both the numerical abundance and body mass of species. We applied both frequentist and Bayesian modeling techniques to empirically estimate the interspecific allometric scaling coefficient (and quantify uncertainty around it) for eDNA production for two groups of fishes represented in the dataset: Northwestern Atlantic marine *Osteichthyans* (bony fishes) and *Chondrichthyans*. We also developed an online tool to facilitate the integration of allometry in eDNA/abundance relationships. Using our tool, researchers can explore how accounting for allometry improves correlations between quantitative eDNA data and organism abundance.

2 | MATERIALS AND METHODS

2.1 | Trawl survey and eDNA collection, extraction, and analysis

For a full description of methodologies used to collect the data, please refer to the original manuscript (Stoeckle et al., 2021). In

brief, eDNA sampling was paired with trawl data collected off the northeastern coast (New Jersey) of the United States for 1-week period in January, June, August, and November in 2019. A minimum of 10 "tows" per three depth intervals for each sampling period were conducted, with a total of 30 traditional trawl samples collected in January and 39 in the other 3 months. For each tow, species identification, number of individuals, and total-mass-per species data were collected. Species accumulation curves (SACs) were used to assess whether trawling captured most available species; SACs were calculated for each month using the R package *vegan* (Oksanen et al., 2020). Visual saturation of SACs indicated that trawling likely captured most available species (Appendix S1, section 1.0).

For each monthly sampling period, two 1 L water samples (one surface and one bottom-depth sample) were collected immediately prior to trawl samples at 10 selected tow sites, for a total target of 20 eDNA samples per sampling month period. Negative tap-water controls were filtered using the same equipment each day of sampling. However, due to bottle breakage and equipment failure, an average of 17 water samples were collected each monthly sampling period. Water samples were maintained on ice and then placed in a −20°C freezer within 24 h of collection, after which they were thawed and filtered using a 0.45 μm nitrocellulose filter, which was stored in a −80°C freezer. DNA was subsequently extracted from the filters using a modified protocol for the PowerSoil kit (Qiagen) (as described in Stoeckle et al., 2020) and extracts were kept frozen prior to library preparation.

DNA processing and bioinformatics were conducted as described in Stoeckle et al. (2020) and Stoeckle et al. (2021). Separate primer sets that target a ~106-bp segment on the mitochondrial 12 S V5 region were used to amplify Northwestern Atlantic bony fishes (*Osteichthyes*) and Cartilaginous fishes (*Chondrichthyes*); each eDNA sample was amplified twice: once with bony fish primer set and once with Cartilaginous fish primer set. Bony and Cartilaginous fish amplifications were indexed separately. Sequencing was performed on an Illumina MiSeq for a total of 136 samples (*Chondrichthyan* and bony fishes per field sample) and 79 negative controls. Bioinformatics analysis was conducted using *DADA2* (Callahan et al., 2016), with taxonomic assignments based on a 100% amplicon sequence variant (ASV) match to a 12S reference library of regional fishes (Stoeckle et al., 2017).

2.2 | Trawl and eDNA data curation

As in Stoeckle et al. (2021), monthly catch weights were normalized by converting catch data to per-tow values; this facilitated comparisons across sampling periods with different total numbers of tows. Read numbers were normalized across seasons with different sampling effort (i.e., total number of collected samples) by converting read counts to per-sample values and multiplying by twenty. All comparisons were done using monthly trawl weights (sum of normalized trawl catches) and monthly eDNA reads (sum of normalized read counts).

Data for Northwestern Atlantic Cartilaginous and bony fishes were analyzed separately for both biological and molecular analysis reasons. First, these two groups have fundamentally different morphological and physiological characteristics that could affect relative eDNA production rates. The surface of *Chondrichthyans*, for example, is characterized by distinct scale morphology and thinner mucous layers compared to bony fishes (Ankhelyi et al., 2018), they possess a distinct excretory system (retention of urea, rectal gland, etc.) (Evans, 2010), and they possess morphologically distinct digestive systems (e.g., spiral valve intestines) (Wetherbee & Gruber, 1993). Furthermore, *Chondrichthyan* DNA was amplified using a different primer set; variation in amplification efficiency between the different primer sets could also impact relative recovery of metabarcoding reads. Collectively, differences in relative eDNA production rates and metabarcoding read recovery could significantly affect the estimation of allometric scaling in eDNA production if data from both taxonomic groups are pooled, particularly given that Chondrichthyan species represented in this dataset were, on average, substantially larger-bodied than bony fishes (mean body size = 11.72 vs. 0.63 kg, respectively). Sea lampreys (*Petromyzon marinus*) were also excluded from both datasets due to their ancient divergence from both taxonomic groups (Gess et al., 2006).

For our analyses, we only considered data for fish species that were detected by eDNA sampling in at least 1 month of the year (i.e., species that were only ever caught in trawls were excluded). Such species were excluded from our analysis because we could not distinguish whether there was no detectable eDNA for these taxa at a given site, or whether the eDNA assay was not capable of detecting these specific taxa (due to potential primer mismatches, etc.). Among bony fishes, Northern Searobin (*Prionotus carolinus*) represented a significant outlier datapoint, with relative biomass catch in the month of August seven times higher than the next highest-catch bony fish species across all sampling periods (111 kg-per-tow vs. 16 kg-per-tow, respectively). Preliminary analyses demonstrated that this singular datum was potentially driving observed relationships and allometric scaling coefficient estimates. The relationship between metabarcoding and original eDNA template concentration can potentially exhibit high residual error due to differences in amplification efficiency across taxa (Elbrecht & Leese, 2015; Kelly et al., 2019; Piñol et al., 2015). Similarly, catch per unit effort (CPUE) can also be a poor index of organism abundance under some circumstances (e.g., hyperstability or hyperdepletion) (Harley et al., 2001; Hubert et al., 2012; Rose & Kulka, 1999). Across a large number of datapoints, correlations between these indexes (metabarcoding reads and CPUE and biomass per unit effort [BPUE]) and the underlying variables they track (eDNA template concentration and organism abundance) are likely to be positive in many scenarios. However, a single outlier datapoint exhibiting a disproportionate effect on the analysis could result from stochastic measurement error associated with index variables in relation to the corresponding indicator variables. For the analyses presented in the main text, Northern Searobin were therefore excluded; results with this species retained are presented in Appendix S1 (section 2.0) for comparison.

2.3 | Statistical analyses

2.3.1 | Integrating allometry into metrics of abundance

Environmental DNA production was assumed to scale allometrically according to the following formula:

$$I = I_0{}^{*} M^{b}$$

Where I = eDNA production rate, M = the individual body mass of an organism, I_0 = a normalization constant, and b = an allometric scaling coefficient.

Allometry was integrated into metrics of fish abundance using the following formula:

$$\mathrm{APT}_i = \left(\overline{x}_i^{b}\right) \bullet N_i$$

Where APT_i = allometrically scaled abundance per tow for the ith species, $\overline{x}_i^{b}$= the mean individual body mass of the ith species, N_i = the mean capture per tow of the ith species, and b = the interspecific allometric scaling coefficient. Note that a value of 0 for b corresponds exactly with species counts per tow, and a value of 1 for b corresponds exactly with species biomass per tow.

We lacked size data for each individual fish, with only total biomass per species and species counts available from tow data. As a result, we employed the simplifying assumption that each individual organism could be represented by the mean mass for that taxon (i.e., biomass per tow [BPT] divided by individuals per tow [IPT]). Although this simplifying assumption may not be suitable across all ecosystems, it is likely a reasonable approximation for our study system. First, in our dataset interspecific variation in body mass is much greater than intraspecific variability in body mass (minimum mean mass = ~1 g [Bay anchovy, *Anchoa mitchilli*], maximum mean mass = 44 kg [Atlantic sturgeon, *Acipenser oxyrhynchus*]). Furthermore, simulations indicate that the level of bias introduced by this assumption is likely small (Appendix S1, section 3.0). Under a uniform distribution with body mass variation ranging from 1 to 100 (largest individuals are 100× larger than the smallest) we found that mean percent bias was <5%. This simulated uniform distribution has much higher variation than our observed data. We were also able to generate some individual body mass distribution data by examining tows where only one individual was captured. For all 15 species for which individual data was available for >10 individuals across sampling months interspecific variation was substantially less than in our simulated dataset (Appendix S1, section 2.0). However, it is important to note that incorporating individual weights may be more important in study systems where interspecific diversity in body mass is low or where there are small numbers of species in which there is considerable overlap in cohorts within habitats (e.g., small freshwater streams).

2.3.2 | Frequentist model

To estimate the optimal value of the scaling coefficient using frequentist regression approaches, we repeated methodologies used in Yates, Glaser, et al. (2021) and Yates, Wilcox, et al. (2021). For each taxonomic group (Northwestern Atlantic bony fishes and Chondrichthyans) we built linear models of eDNA metabarcoding read counts as a function of allometrically scaled abundance per tow (APT^{b}) with scaling coefficient values (b) ranging from 0.00 to 1.00 by 0.01 intervals. We then extracted Akaike Information Criterion (AIC; Akaike, 1974) for each model; we predict that the distribution of AIC values corresponding to values of b between 0.00 and 1.00 should follow an approximate concave parabolic distribution, with a "best-fit" (i.e., lowest-AIC) scaling coefficient value occurring at the "vertex" of this approximate parabola (Yates, Glaser, et al., 2021). AIC and model *RMSE* values were compared for the "optimal" scaling coefficient model and two traditional metrics of organism abundance: density (i.e., individuals-per-tow, or "IPT") and biomass (i.e., biomass per tow, or "BPT").

Visual inspection of biplots indicated residual heteroscedasticity in quantitative eDNA data as APT^{b} increased. As a result, we used the *gls* function from the package *nlme* to fit a generalized least-squares model that utilized the varPower variance function to fit a heteroscedastic residual error term associated with the APT^{b} variable. This function cannot tolerate APT^{b} values equal to zero—as a result, a value of 0.001 was added to all zero values for "individuals-per-tow." To evaluate the significance of the heteroscedastic error term, AIC values for the "optimal" APT^{b}, IPT, and BPT were compared to models without the additional residual variance function. All analyses were conducted in *R* v. 4.0.4 (R Core Team, 2019).

2.3.3 | Bayesian model

For Bayesian analysis, we considered the regression model below where c_0 is the regression intercept, APT^{b} follows the form in Equation (2), c_1 is the regression slope, and ε is the variance:

$$\text{Read count} \sim \mathrm{Norm}\left(c_0 + \mathrm{APT}^{b} \times c_1, \varepsilon\right) \quad (1.3)$$

We built separate models for Northwestern Atlantic bony fishes and Cartilaginous fishes and implemented Markov Chain Monte Carlo (MCMC) simulations in *JAGS* (Plummer, 2003) using the *rjags* (Denwood, 2016) and *jagsUI* (Kellner, 2021) packages in *R*. For each model, we ran three parallel chains for 5,000,000 total iterations, discarding the first 50,000 for burn-in and thinning to every 500th iteration to estimate the posterior distribution for each parameter and derive 95% Bayesian Credible Intervals (BCI). We assessed convergence based on a value of $\widehat{R} < 1.1$ (Gelman & Rubin, 1992). We used uniform priors for the latent b (0–1 for bony fishes and 0–2 for Chondrichthyans based on frequentist modeling results; see Results), intercept ($0–10^{6}$), beta

($0–10^5$), and ε ($0–10^3$ terms) parameters and initial values estimated from the frequentist regression models. An additional heteroscedastic residual error term was fitted that allowed residual error to vary as a power function of APT^b (uniform prior = 0–1), with the significance of the heteroscedastic error term evaluated by comparing model DIC to a model lacking the heteroscedastic variance term.

3 | RESULTS

3.1 | Northwestern Atlantic bony fishes

Northwestern Atlantic Bony fish species' IPT and BPT were significantly and positively correlated with eDNA metabarcoding read counts (Table 2, Figure 1). The distribution of AIC values from the frequentist models exhibited the predicted approximate upward parabolic distribution (Figure 2). The "optimal" AIC value corresponded to a scaling coefficient point estimate (*b*) of 0.78 and represented a significant improvement over IPT and BPT (ΔAIC = 71.20 and 8.26, respectively). Similarly, $APT^{0.78}$ exhibited substantially lower Root Mean Square Error (Table 1). Values for *b* between 0.69 and 0.88 had AIC values within two of the "optimal" AIC value. In all cases, including a heteroscedastic residual error term associated with fish abundance significantly improved model fit (ΔAIC > 100 for all models).

Values from the frequentist model with a scaling coefficient of 0.78 were used to initialize parameter values for the Bayesian model, although model results were largely unaffected by initial parameter values. The Bayesian model converged successfully and we derived a point estimate for the scaling coefficient of 0.77 with a 95% credible interval of 0.64–0.92 (Figure S1), exhibiting close correspondence to the frequentist approach (Figure 2). Similar to the above analysis, inclusion of a power-function heteroscedastic error term associated with APT significantly improved model fit (ΔDIC = 104.2).

Analyses above removed Northern Searobin, which was a high leverage outlier datum. Analyses of bony fish data with Northern Searobin included still found evidence of allometric scaling; the point estimates for the scaling coefficient using frequentist approaches and Bayesian methods were 0.80 and 0.77 (Bayesian estimate credible interval = 0.57–0.97), respectively (see Appendix S1, section 3.0). Allometric scaling in eDNA production was therefore still observed/inferred regardless of whether this outlier species was included.

3.2 | Chondrichthyes

Northwest Atlantic Chondrichthyan species' BPT was significantly and positively correlated with eDNA metabarcoding read counts, although IPT was not (see Table 2, Figure 3). The distribution of AIC values from the frequentist models with scaling coefficient values ranging from 0.00 to 1.00 did not exhibit the predicted upward parabolic distribution; AIC values instead declined as scaling coefficients approached BPT (*b* = 1.00). We therefore explored the effect of scaling coefficient values >1.00. The predicted "approximate" upward parabolic distribution of AIC values was only observed when scaling coefficient values were extended to 2.00 (Figure 4). The "optimal" AIC value corresponded to a scaling coefficient value of 1.49, implying that large-bodied *Chondrichthyans* had higher mass-specific eDNA production rates than smaller *Chondrichthyans*; this model represented a significant improvement over IPT and BPT (ΔAIC = 11.75 and 3.30, respectively), with lower associated RMSE values (Table 2). In all cases, including a heteroscedastic residual error term associated with Northwest Atlantic Chondrichthyan abundance significantly improved model fit (ΔAIC > 50 for all models).

Values from the frequentist model with a scaling coefficient of 1.49 were used to initialize parameter values for the Bayesian model. We derived a point estimate for the scaling coefficient from the Bayesian model of 0.94, a considerable discrepancy from the frequentist model (Figures 4 and S2). The Bayesian model, however, did not converge successfully regardless of initialized parameter values (i.e., $\widehat{R} > 1.10$), with inconsistent posterior distributions that were variable between chains (Figure S2).

4 | DISCUSSION

We found that eDNA shedding rates scaled allometrically (i.e., larger fish produce less eDNA per unit body mass) across

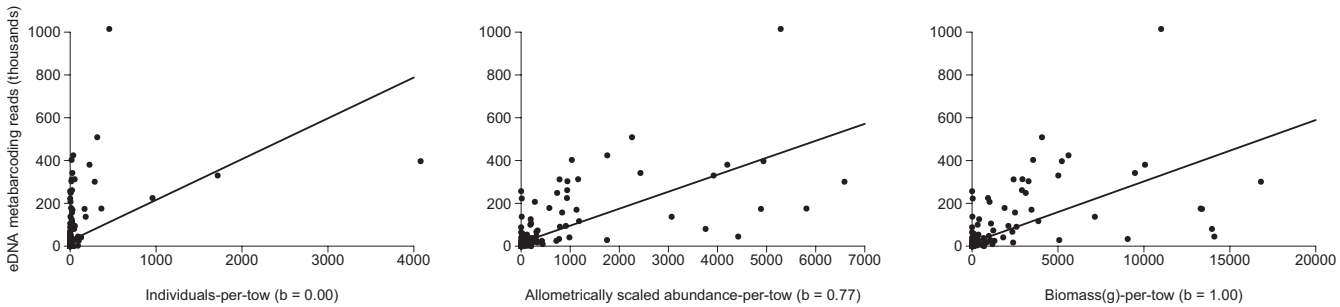

FIGURE 1 Linear regressions for bony fish species' eDNA metabarcoding read count (thousands) and three metrics of abundance: (a) Individuals-per-tow, (b) Allometricallyscaled abundance per tow (*b* = 0.77) ($APT^{0.77}$), and (c) Biomass per tow. Note that the scaling coefficient estimate represented in figure (b) was the point estimate derived from the Bayesian model

Northwestern Atlantic bony fish species in a natural system. This is an important observation because when researchers correlate quantitative eDNA data with traditional metrics of organism abundance (e.g., numerical abundance or biomass) they make implicit assumptions about the value of the allometric scaling coefficient (*b*); correlating eDNA data with density assumes a scaling coefficient value of "0" and with biomass assumes a scaling coefficient value of "1." Further research is needed to test the generality of our findings across systems, but this work demonstrates (1) that it is possible to infer interspecific allometric scaling coefficients from large observational datasets of paired eDNA metabarcoding and animal capture data in natural ecosystems and (2) that incorporating an understanding of allometric scaling may strengthen correlations between read count data and organism abundance. Although interspecific allometry in eDNA production should also be experimentally validated under controlled conditions, large-scale observational datasets represent valuable opportunities to explore the fundamental "ecology" of eDNA production in natural ecosystems. Future large-scale studies should similarly attempt to infer whether allometrically scaling processes may be affecting the distribution of eDNA in natural ecosystems.

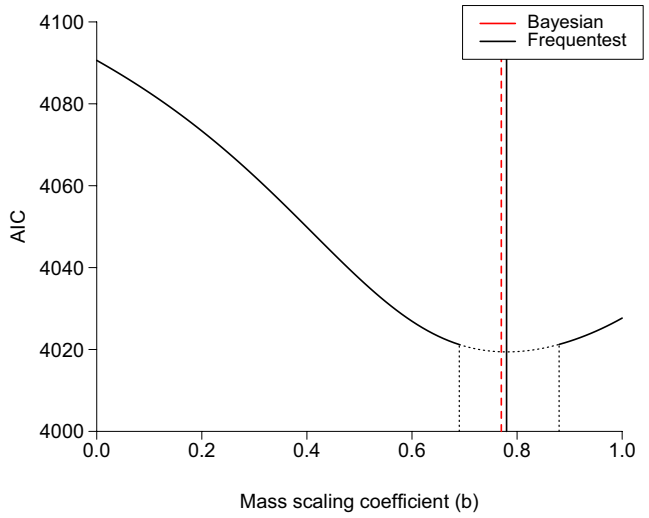

FIGURE 2 Distribution of AIC values for linear regressions between bony fish abundance and eDNA metabarcoding read count, corresponding to scaling coefficients ranging from 0.00 to 1.00. The dotted portion of the curve denoted with vertical dotted lines denotes the range of models with ΔAIC < 2 of the "optimal" scaling coefficient model. The black vertical line represents the best-fit scaling coefficient estimated using frequentist approaches, and the red vertical line represents the best-fit scaling coefficient estimated using the Bayesian model

We note, however, that our findings herein are taxa and ecosystem-specific; our findings apply only to Northwestern Atlantic bony fish species, and the extent to which they can be generalized to other taxonomic groups and/or ecosystems is presently unknown. We posit that our findings are *likely* to be generalizable to other study systems because the inferred value of *b* is close to expected values based on theory. However, more studies examining relationships between eDNA, organism abundance, and allometry are required before broad generalizations can be made. In particular, a meta-analysis of published datasets could elucidate the contexts in which allometry is likely to impact pseudo-steady-state concentrations of eDNA in an environment. To this end, we encourage future studies examining the relationships between quantitative eDNA data and organism abundance to integrate allometry; any study that has both numerical abundance and biomass data can employ the methods presented herein. At the very least, we encourage studies to report data and correlations with eDNA for both numerical abundance and biomass, rather than just reporting only the traditional abundance metric that "fits best" with quantitative eDNA data (i.e., produces the highest r^2 value).

To further facilitate the integration of allometry into other eDNA/abundance studies, we developed an online tool (https://nationalgenomicscenter.shinyapps.io/InterspecificASM/) that allows users to upload their own data and explore how different assumed values of "b" change the association between ASM-corrected quantitative eDNA data and metrics of abundance and biomass based on conventional sampling. This tool can accommodate data from both intraspecific (e.g., eDNA concentrations assess by qPCR for a single species

Model	*F*	*p*	AIC	ΔAIC	RMSE
IPT	$12.12_{(1158)}$	<0.001	4090.61	71.20	121575.1
BPT	$56.09_{(1158)}$	<0.001	4027.67	8.26	104888.7
$APT^{0.78}$	$78.17_{(1158)}$	<0.001	4019.41	-	94726.4

Note: ΔAIC represents the difference in AIC value between $APT^{0.78}$ And the IPT and BPT models. Note that these results are for analyses in which northern Searobin was excluded.

TABLE 1 Frequentist results for generalized least-squares regressions between eDNA metabarcoding read count and individuals per tow (IPT), biomass per tow (BPT), and allometrically scaled abundance per tow (APT, $b = 0.78$) for bony fish

Model	*F*	*p*	AIC	ΔAIC	RMSE
IPT	$1.76_{(1,35)}$	0.192	994.78	11.75	593992.7
BPT	$14.25_{(1,35)}$	0.001	986.33	3.30	360878.7
$APT^{1.49}$	$35.15_{(1,35)}$	<0.001	983.03	–	284065.0

Note: ΔAIC represents the difference in AIC value between $APT^{1.49}$ And the IPT and BPT models.

TABLE 2 Frequentist results for generalized least-squares regressions between eDNA concentration and individuals per tow (IPT), biomass per tow (BPT), and allometrically scaled abundance per tow (APT, $b = 1.49$) for Chondrichthyans

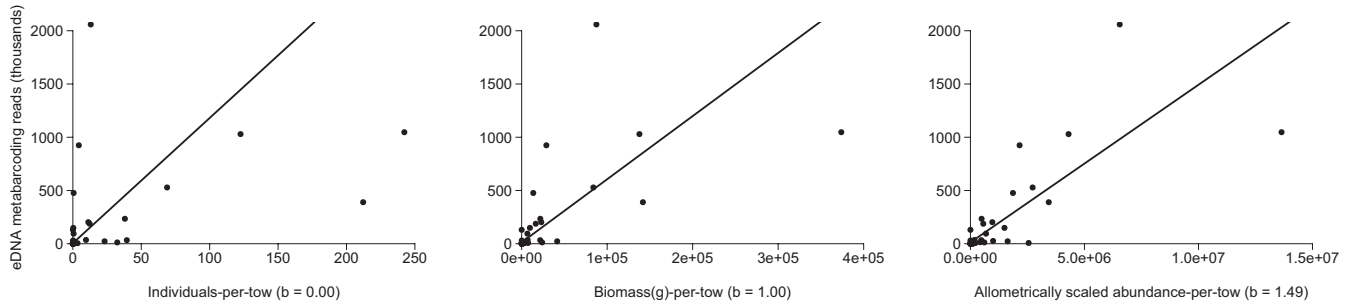

FIGURE 3 Linear regressions for Chondrichthyan species' eDNA metabarcoding read count (thousands) and three metrics of abundance: (a) Individuals per tow, (b) Allometrically scaled abundance per tow ($b = 1.49$) ($APT^{1.49}$), and (c) Biomass per tow. Note that the scaling coefficient estimate represented in figure (b) was the point estimate derived from the frequentist model as our Bayesian model failed to converge

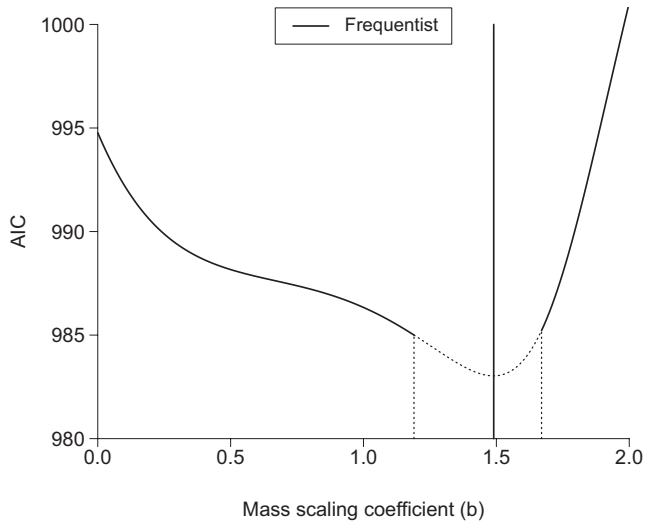

FIGURE 4 Distribution of AIC values for linear regressions between Cartilaginous fish abundance and eDNA metabarcoding read count, corresponding to scaling coefficients ranging from 0.00 to 2.00. The dotted portion of the curve denoted with vertical dotted lines denotes the range of models with $\Delta AIC < 2$ of the "optimal" scaling coefficient model. The black vertical line represents the best-fit scaling coefficient estimated using frequentist approaches; note that the Bayesian model point estimate was 0.94, but the model failed to converge

across multiple environments) and interspecific (e.g., quantitative metabarcoding read counts for multiple species) studies. Users can upload quantitative eDNA data, numerical abundance, and mean population/species body mass data; in this case, the tool will assume that organisms from the same biological replicate/population/species (depending on study system) have identical body mass values (as herein). Alternatively, users can provide individual body mass data derived from a subsample or complete census of individuals from a biological replicate/population/species, in which case the tool will calculate "allometrically scaled mass" using the following formula (as in Yates, Glaser, et al., 2021; Yates, Wilcox, et al., 2021):

$$\mathrm{ASM} = \frac{\sum_{i=1}^{N_S} \left(\mathrm{mass}_{Si}^{b}\right)}{N_S} \bullet \hat{N}$$

Where $\sum_{i=1}^{N_S} \left(mass_{Si}^{b}\right)$ is the sum of the individual mass values raised to the power of a scaling coefficient (b) in the subset or census of individuals used to assess biological replicate/population/species size structure, N_S is the number of fish captured in the subset/census, and $\hat{N}$ is the estimated population size. This methodology assumes that the size structure assessment was representative of the biological replicate/population/species when a subset of individuals was sampled.

Overall, we found empirical evidence that the value of b for Northwestern Atlantic bony fish eDNA production corresponds closely to theoretical expectations based on whole-body surface area allometry and allometry in key physiological and metabolic rates. Stoeckle et al. (2021) investigated the effect of allometry on eDNA production by fixing the value of b in their "allometric abundance index" to 2/3 based on these theoretical expectations; this appears to have been a reasonable approximation, given that our empirically derived point estimate for the value of b for Northwestern Atlantic bony fishes corresponded to 0.78 with credible intervals that overlapped with 2/3, although it is important to note that this is likely a "conservative" estimate of the credible interval (i.e., intervals may be larger) due to the fact that the independent variable in the analysis (organism abundance) was also estimated with error, rather than experimentally controlled (e.g., as in a mesocosm experiment). Nevertheless, the point estimate and credible intervals we obtained corresponded approximately to allometric scaling rates observed for body surface area in fish ($b \sim 0.60–0.65$) (O'Shea et al., 2006), metabolic rates (e.g., $b = 0.75$) (Brown et al., 2004), and for key physiological rates like consumption/excretion/egestion (Allegier et al., 2015; Post et al., 1999; Vanni & McIntyre, 2016; Wiff & Roa-Ureta, 2008). Notably, credible intervals also overlapped with a recently derived empirical estimate of 0.89 (0.82–0.99) for the value of the metabolic scaling coefficient in fishes (Jerde et al., 2019).

Furthermore, while common Bayesian modeling packages can provide the modeling flexibility to directly estimate non-linear model parameters and their error, they are also useful because "informative priors" can be used to shape models when insufficient data are available to directly estimate coefficients. If allometry in eDNA production is validated more broadly, smaller-scale studies that lack the sample size to accurately estimate scaling coefficients

directly could potentially use informative priors based on previous work and potentially strengthen resulting eDNA/abundance correlations. We also note that the Bayesian modeling approaches utilized herein produced very similar point estimates to the AIC-based approaches utilized in previous studies (e.g., Yates, Glaser, et al., 2021), but likely provide more rigorous estimates of uncertainty around the *b*-parameter estimate.

We do note, however, that we anticipate that the value of integrating allometry to abundance/eDNA concentration correlations will be lower with smaller metabarcoding datasets (e.g., <~15–20 species). A number of factors (e.g., differences in PCR efficiency among species [Elbrecht & Leese, 2015; Leese et al., 2021], community composition [Piñol et al., 2019]) can potentially introduce substantial "noise" into the relationship between quantitative eDNA read data and organism abundance (Kelly et al., 2019; Yates, Cristescu, & Derry, 2021). In large datasets with adequate sample size of species (i.e., >~20 species), such "noise" may "average out" such that a biologically meaningful signal is detectable; in small datasets, stochastic idiosyncrasy in amplification efficiency among taxa may well "drown out" allometric effects of eDNA production. Advances in metabarcoding that improve the relationship between read count and original template eDNA concentrations (e.g., correcting for taxa-specific amplification efficiency (Kelly et al., 2019)) could potentially improve the utility of correcting for allometry. At the very least, however, future studies should explore the utility of transforming abundance data using scaling coefficients derived from theoretical expectations; a scaling coefficient value of approximately 0.66–0.75 (i.e., as predicted from surface area, excretion, and metabolic allometry) appears to be justifiable as an approximation, but its consistency and broader applicability across other study systems requires further study.

Understanding the physiological processes involved in eDNA production also has potential implications for the application of eDNA for monitoring. Although model predictive power was low overall, integrating allometry (i.e., $APT^{0.78}$) helped linearize eDNA/abundance data and significantly improved model predictive capacity, as indicated by RMSE values, relative to models based on traditional metrics. The linear relationship between organism abundance and read count we observed was weaker than typically observed for single-species qPCR/dPCR approaches (Yates et al., 2019), likely due to (previously discussed) factors in metabarcoding that can introduce "noise" in the relationship between read count and template eDNA concentrations (Yates, Cristescu, & Derry, 2021). Our results, however, suggest that the physiology of eDNA production may be an important consideration for metabarcoding studies attempting to infer relative organism abundance from eDNA read count.

Scaling factors and constants, however, may need to be specific to taxonomic/phylogenetic groups because physiological processes involved in eDNA production are complex and likely variable across species and taxonomic groups (Sassoubre et al., 2016; Yates, Cristescu, & Derry, 2021). Northwestern Atlantic bony fishes and *Chondrichthyans*, for example, exhibit substantial differences in physiology and morphology that could impact relative eDNA production and, thus, cross-taxonomic allometric relationships in eDNA production. Similarly, physiological processes among specific taxa could also result in a breakdown of typical allometric relationships in eDNA production. Reproductive activity (e.g., broadcast spawning) can result in an increase in mass-specific eDNA production rate (Curtis et al., 2020; Takeuchi et al., 2019); accounting for reproductive activities during eDNA sample collection timing could be relevant, particularly for species that might appear as "outliers" with larger than expected mass-specific eDNA production rates. Variability in primer amplification efficiency (both within and between primer sets) might also limit inter-taxa comparisons between read counts and organism abundance (Elbrecht & Leese, 2015; Kelly et al., 2019). Accounting for phylogeny may therefore be important when conducting such comparisons across broad taxonomic groups.

While Northwestern Atlantic bony fishes exhibited patterns corresponding to theoretical expectations, it is important to note that Chondrichthyans deviated substantially from predictions, with frequentist approaches provided a scaling coefficient estimate of 1.49 and our Bayesian models failing to converge. While this may be indicative of a potential biological phenomenon warranting further study, the more likely explanation is that we simply lacked the statistical sample size/power to estimate the value of the scaling factor from potentially "noisy" metabarcoding/trawl data; with only 13 species and 37 datapoints, the Chondrichthyan dataset had significantly lower representation relative to bony fish (with 56 species with 160 datapoints). Quantitative metabarcoding data may be particularly "noisy" given that variability among amplification efficiency can be common even among closely related taxa in metabarcoding (Elbrecht & Leese, 2015; Piñol et al., 2015). This amplification efficiency variability could thus introduce potential residual error in the relationship between metabarcoding read count and organism abundance due to imperfect correlation between final read count and the original template eDNA concentrations. Catch per unit effort (CPUE) data can also be poorly correlated with abundance for some species and systems (Harley et al., 2001; Hubert et al., 2012; Rose & Kulka, 1999; Yates, Glaser, et al., 2021). As a result, error between our index variables (read count and CPUE/BPUE data) and underlying fundamental parameters (eDNA concentration and organism abundance), combined with small sample size, could potentially account for both the unusual results we observed for Chondrichthyans and the failure of our Bayesian model to converge even with model parameters initialized based on the frequentist model.

5 | CONCLUSIONS AND RECOMMENDATIONS

Our findings demonstrate that considering the physiology of eDNA production may be important for the future application of eDNA sampling to monitor organism abundance. Understanding the consistency of the effect of allometric processes on eDNA production, as well as conditions under which allometric patterns might emerge,

is crucial for evaluating the extent to which integrating allometry can improve eDNA/abundance correlations and, ultimately, help operationalize eDNA to monitor abundance and biodiversity in natural ecosystems. The extent to which our findings might apply to other ecosystems remains unknown; a meta-analysis of other datasets could potentially address this consistency of the potential impact of allometry on eDNA production across different contexts. We therefore encourage future studies to consider the implicit assumptions regarding the physiology of eDNA production made correlating eDNA with species *N* and biomass. To this end, we encourage users to explore the effect of integrating allometry on the relationship between eDNA and organism abundance using the online tool we developed (https://nationalgenomicscenter.shinyapps.io/InterspecificASM/).

We also want to re-emphasize that correlating quantitative eDNA data exclusively to traditional metrics of organism abundance (e.g., *N* and biomass) makes inherent assumptions regarding the physiology of eDNA production, regardless of whether researchers explicitly consider or evaluate the value of the allometric scaling coefficient (*b*) within their own study systems; comparing eDNA to *N* or biomass simply fixes the assumed value of *b* at 0 or 1, respectively. Future researchers should explicitly consider and evaluate how they might expect eDNA production to scale allometrically within and across species—is eDNA production likely to be a function of numerical abundance (i.e., $b = 0$), biomass (i.e., $b = 1$), or something in between (i.e., $0 < b > 1$)? In particular, we would encourage future studies to consider allometry in study systems where populations or species exhibit substantial variation in body size distributions; allometry is unlikely to affect relative eDNA production rates when organisms exhibit similar body sizes across groups (i.e., populations or species). Understanding the consistency of the effect of allometric processes on eDNA production, as well as conditions under which allometric patterns might emerge, is crucial for evaluating the extent to which integrating allometry can improve eDNA/abundance correlations and, ultimately, help operationalize eDNA to monitor abundance in natural ecosystems.

AUTHOR CONTRIBUTIONS

M. C. Yates and T. W. Wilcox analyzed the dataset and wrote the initial draft of the manuscript. M. Y. Stoeckle provided the raw data for analysis and advised on the construction of the dataset. All authors provided conceptual contributions to the manuscript and contributed substantially to subsequent drafts.

ACKNOWLEDGMENTS

We would like to thank Adam Sepulveda, whose review of our manuscript greatly improved subsequent versions and whose ideas and commentary opened up a number of new avenues to explore. M. C. Yates was funded by a CIGLR and NSERC postdoctoral fellowship.

CONFLICT OF INTEREST

The authors have no conflict of interest.

DATA AVAILABILITY STATEMENT

No new data were generated in this manuscript; data were obtained from Stoeckle et al. (2021). Curated datasets can be found in the Dryad digital repository, at: https://doi.org/10.5061/dryad.rxwdbrvd0

ORCID

Matthew C. Yates https://orcid.org/0000-0002-9199-1078
Taylor M. Wilcox https://orcid.org/0000-0003-3341-7374

REFERENCES

Akaike, H. (1974). A new look at the statistical model identification. *IEEE Transactions on Automatic Control*, *19*, 716–723.

Allegier, J. E., Wenger, S. J., Rosemond, A. D., Schindler, D. E., & Layman, C. A. (2015). Metabolic theory and taxonomic identity predict nutrient recycling in a diverse food web. *PNAS*, *112*(20), E2640–E2647. https://doi.org/10.1073/pnas.1420819112

Ankhelyi, M. V., Wainwright, D. K., & Lauder, G. V. (2018). Diversity of dermal denticle structure in sharks: Skin surface roughness and three-dimensional morphology. *Journal of Morphology*, *279*(8), 1132–1154. https://doi.org/10.1002/jmor.20836

Barnes, M. A., & Turner, C. R. (2016). The ecology of environmental DNA and implications for conservation genetics. *Conservation Genetics*, *17*(1), 1–17. https://doi.org/10.1007/s10592-015-0775-4

Brown, J. H., Gillooly, J. F., Allen, A. P., Savage, V., & West, G. B. (2004). Toward a metabolic theory of ecology. *Ecology*, *85*(7), 1771–1789.

Callahan, B.J., McMurdie, P.J., Rosen, M.J., Han, A.W., Johnson, A.J.A., and Holmes, S.P. 2016. DADA2: High-resolution sample inference from Illumina amplicon data. *Nature Methods 13*(7): 581–583. Nature Publishing Group. doi:https://doi.org/10.1038/nmeth.3869

Cristescu, M. E. (2014). From barcoding single individuals to metabarcoding biological communities: Towards an integrative approach to the study of global biodiversity. *Trends in Ecology & Evolution*, *29*(10), 566–571. https://doi.org/10.1016/j.tree.2014.08.001

Curtis, A. N., Tiemann, J. S., Douglass, S. A., Davis, M. A., & Larson, E. R. (2020). High stream flows dilute environmental DNA (eDNA) concentrations and reduce detectability. *Diversity and Distributions Early View*, *27*, 1918–1931. https://doi.org/10.1111/ddi.13196

Denwood, M. (2016). runjags: An R package providing interface utilities, model templates, parallel computing methods and additional distributions for MCMC models in JAGS. *Journal of Statistical Software*, *71*, 1–25.

Elbrecht, V., & Leese, F. (2015). Can DNA-based ecosystem assessments quantify species abundance? Testing primer bias and biomass-sequence relationships with an innovative metabarcoding protocol. *PLoS One*, *10*(7), e0130324. https://doi.org/10.1371/journal.pone.0130324

Evans, D. H. (2010). A brief history of the study of fish osmoregulation: The central role of the Mt. Desert Island biological laboratory. *Frontiers in Physiology*, *1*(6), 1–10. https://doi.org/10.3389/fphys.2010.00013

Evans, N. T., Olds, B. P., Renshaw, M. A., Turner, C. R., Li, Y., Jerde, C. L., Mahon, A. R., Pfrender, M. E., Lamberti, G. A., & Lodge, D. M. (2016). Quantification of mesocosm fish and amphibian species diversity via environmental DNA metabarcoding. *Molecular Ecology Resources*, *16*, 29–41. https://doi.org/10.1111/1755-0998.12433

Gelman, A., & Rubin, D. B. (1992). Inference from iterative simulation using multiple sequences. *Statistical Science*, *7*(4), 457–472.

Gess, R. W., Coates, M. I., & Rubidge, B. S. (2006). A lamprey from the Devonian period of South Africa. *Nature*, *443*(7114), 981–984. https://doi.org/10.1038/nature05150

Hanfling, B., Handley, L. L., Read, D. S., Hahn, C., Li, J., Nichols, P., Blackman, R. C., Oliver, A., & Winfield, I. J. (2016). Environmental DNA metabarcoding of lake fish communities reflects long-term data from established survey methods. *Molecular Ecology*, *25*, 3101–3119. https://doi.org/10.1111/mec.13660

Harley, S. J., Myers, R. A., & Dunn, A. (2001). Is catch-per-unit-effort proportional to abundance? *Canadian Journal of Fisheries and Aquatic Sciences*, *58*(9), 1760–1772. https://doi.org/10.1139/cjfas-58-9-1760

Hubert, W., Pope, K. L., & Dettmers, J. M. (2012). Passive capture techniques. In A. V. Zale, D. L. Parrish, & T. Sutton (Eds.), *Fisheries techniques* (3rd ed.). American Fisheries Society.

Jerde, C. L., Kraskura, K., Eliason, E. J., Csik, S. R., Stier, A. C., & Taper, M. L. (2019). Strong evidence for an intraspecific metabolic scaling coefficient near 0.89 in fish. *Frontiers in Physiology*, *10*(9), 1–17. https://doi.org/10.3389/fphys.2019.01166

Kellner, K. (2021). jagsUI: A wrapper around "rjags" to streamline "JAGS" analyses.

Kelly, R. P., Shelton, A. O., & Gallego, R. (2019). Understanding PCR processes to draw meaningful conclusions from environmental DNA studies. *Scientific Reports*, *9*(1), 1–14. https://doi.org/10.1038/s41598-019-48546-x

Lamb, P. D., Hunter, E., Pinnegar, J. K., Creer, S., Davies, R. G., & Taylor, M. I. (2019). How quantitative is metabarcoding: A meta- analytical approach. *Molecular Ecology*, *28*, 420–430. https://doi.org/10.1111/mec.14920

Lawson Handley, L., Read, D. S., Winfield, I. J., Kimbell, H., Johnson, H., Li, J., Hahn, C., Blackman, R., Wilcox, R., Donnelly, R., Szitenberg, A., & Hänfling, B. (2019). Temporal and spatial variation in distribution of fish environmental DNA in England's largest lake. *Environmental DNA*, *1*(1), 26–39. https://doi.org/10.1002/edn3.5

Leese, F., Sander, M., Buchner, D., Elbrecht, V., Haase, P., & Zizka, V. M. A. (2021). Improved freshwater macroinvertebrate detection from environmental DNA through minimized nontarget amplification. *Environmental DNA*, *3*(1), 261–276. https://doi.org/10.1002/edn3.177

Maruyama, A., Nakamura, K., Yamanaka, H., Kondoh, M., & Minamoto, T. (2014). The release rate of environmental DNA from juvenile and adult fish. *PLoS One*, *9*(12), e114639. https://doi.org/10.1371/journal.pone.0114639

Meeh, K. (1879). Oberflachenmessungen des men- schlichen Korpers. *Zeitschrift für Biologie*, *15*, 425–428.

Oksanen, J., Guillaume Blanchet, F., Friendly, M., Kindt, R., Legendre, P., McGlinn, D., Minchin, P. R., O'Hara, R. B., Simpson, G. L., Solymos, P. H., Stevens, M. H. H., Szoecs, E., & Wagner, H. (2020). vegan: community ecology package. Available at: https://cran.r-project.org/package=vegan%0A.

O'Shea, B., Mordue-Luntz, A. J., Fryer, R. J., Pert, C. C., & Bricknell, I. R. (2006). Determination of the surface area of a fish. *Journal of Fish Diseases*, *29*(7), 437–440. https://doi.org/10.1111/j.1365-2761.2006.00728.x

Piñol, J., Mir, G., Gomez-Polo, P., & Agustí, N. (2015). Universal and blocking primer mismatches limit the use of high-throughput DNA sequencing for the quantitative metabarcoding of arthropods. *Molecular Ecology Resources*, *15*(4), 819–830. https://doi.org/10.1111/1755-0998.12355

Piñol, J., Senar, M. A., & Symondson, W. O. C. (2019). The choice of universal primers and the characteristics of the species mixture determine when DNA metabarcoding can be quantitative. *Molecular Ecology*, *28*(2), 407–419. https://doi.org/10.1111/mec.14776

Plummer, M. (2003). JAGS: A program for analysis of Bayesian graphical models using Gibbs sampling JAGS: Just another Gibbs sampler. In DSC 2003 Working Papers.

Post, J. R., Parkinson, E. A., & Johnston, N. T. (1999). Density-dependent processes in structured fish populations: Interaction strengths in whole-lake experiments. *Ecological Monographs*, *69*(2), 155–175. https://doi.org/10.1890/0012-9615(1999)069[0155:DDPISF]2.0.CO;2

R Core Team. (2019). *A language and environment for statistical computing* (Vol. *2*). R Foundation of Statistical Computing Available at: http://www.r-project.org.

Reynolds, P. S. (1996). Phylogenetic analysis of surface areas of mammals. *Journal of Mammalogy*, *78*, 859–868.

Rose, G. A., & Kulka, D. W. (1999). Hyperaggregation of fish and fisheries: How catch-per-unit-effort increased as the northern cod (*Gadus morhua*) declined. *Canadian Journal of Fisheries and Aquatic Sciences*, *56*, 118–127.

Rourke, M. L., Fowler, A. M., Hughes, J. M., Broadhurst, M. K., Dibattista, J. D., Fielder, S., Wilkes, J., & Elise, W. (2021). Environmental DNA (eDNA) as a tool for assessing fish biomass: A review of approaches and future considerations for resource surveys. *Environmental DNA Early View*, *1–25*, 9–33. https://doi.org/10.1002/edn3.185

Sassoubre, L. M., Yamahara, K. M., Gardner, L. D., Block, B. A., & Boehm, A. B. (2016). Quantification of environmental DNA (eDNA) shedding and decay rates for three marine fish. *Environmental Science & Technology*, *50*(19), 10456–10464. https://doi.org/10.1021/acs.est.6b03114

Stoeckle, M. Y., Adolf, J., Charlop-powers, Z., Dunton, K. J., Hinks, G., & Vanmorter, S. M. (2021). Trawl and eDNA assessment of marine fish diversity, seasonality, and relative abundance in coastal New Jersey, USA. *ICES Journal of Marine Science*, *78*(1), 293–304. https://doi.org/10.1093/icesjms/fsaa225

Stoeckle, M. Y., Das Mishu, M., & Charlop-Powers, Z. (2020). Improved environmental DNA reference library detects overlooked marine fishes in New Jersey, United States. *Frontiers in Marine Science*, *7*, 226. https://doi.org/10.3389/fmars.2020.00226

Stoeckle, M. Y., Soboleva, L., & Charlop-powers, Z. (2017). Aquatic environmental DNA detects seasonal fish abundance and habitat preference in an urban estuary. *PLoS One*, *12*, e0175186.

Taberlet, P., Coissac, E., Pompanon, F., Brochmann, C., & Willerslev, E. (2012). Towards next-generation biodiversity assessment using DNA metabarcoding. *Molecular Ecology*, *21*, 2045–2050.

Takeuchi, A., Iijima, T., Kakuzen, W., Watanab, S., & Yamada, Y. (2019). Release of eDNA by different life history stages and during spawning activities of laboratory-reared Japanese eels for interpretation of oceanic survey data. *Scientific Reports*, *9*, 6074. https://doi.org/10.1038/s41598-019-42641-9

Vanni, M. J., & McIntyre, P. B. (2016). Predicting nutrient excretion of aquatic animals with metabolic ecology and ecological stoichiometry: A global synthesis. *Ecology*, *97*(12), 3460–3471. https://doi.org/10.1002/ecy.1582

Wetherbee, B. M., & Gruber, S. H. (1993). Absorption efficiency of the lemon shark Negaprion brevirostris at varying rates of energy intake. *Copeia*, *1993*(2), 416. https://doi.org/10.2307/1447140

Wiff, R., & Roa-Ureta, R. (2008). Predicting the slope of the allometric scaling of consumption rates in fish using the physiology of growth. *Marine and Freshwater Research*, *59*(10), 912–921. https://doi.org/10.1071/MF08053

Yates, M. C., Cristescu, M. E., & Derry, A. M. (2021). Integrating physiology and environmental dynamics to operationalize environmental DNA (eDNA) as a means to monitor freshwater macro-organism abundance. *Molecular Ecology*, *30*(24), 6531–6550.

Yates, M. C., Fraser, D. J., & Derry, A. M. (2019). Meta-analysis supports further refinement of eDNA for monitoring aquatic species-specific abundance in nature. *Environmental DNA*, *1*, 5–13. https://doi.org/10.1002/edn3.7

Yates, M., Glaser, D., Post, J., Cristescu, M., Fraser, D., & Derry, A. (2021). The relationship between eDNA particle concentration and organism abundance in nature is strengthened by allometric scaling. *Molecular Ecology*, *30*, 3068–3082. https://doi.org/10.1111/mec.15543

Yates, M. C., Wilcox, T. M., McKelvey, K. S., Young, M. K., Schwartz, M. K., & Derry, A. M. (2021). Allometric scaling of eDNA production in stream-dwelling brook trout (Salvelinus fontinalis) inferred from population size structure. *Environmental DNA*, *3*(3), 553–560. https://doi.org/10.1002/edn3.150

SUPPORTING INFORMATION

Additional supporting information can be found online in the Supporting Information section at the end of this article.

How to cite this article: Yates, M. C., Wilcox, T. M., Stoeckle, M. Y., & Heath, D. D. (2022). Interspecific allometric scaling in eDNA production among northwestern Atlantic bony fishes reflects physiological allometric scaling. *Environmental DNA*, *00*, 1–11. https://doi.org/10.1002/edn3.381